J. Mendez, P. Violan,* and G. Gasc**

Initiation and Growth of Surface Microcracks in Polycrystalline Copper Cycled in Air and in Vacuum

REFERENCE Mendez, J., Violan, P., and Gasc, C. **Initiation and growth of surface microcracks in polycrystalline copper cycled in air and in vacuum**, *The Behaviour of Short Fatigue Cracks*, EGF Pub. 1(Edited by K. J. Miller and E. R. de los Rios) 1986, Mechanical Engineering Publications, London, pp. 145–161.

ABSTRACT Quantitative information has been obtained on the initiation and early growth of surface microcracks in polycrystalline copper fatigued in air and in vacuum at two different testing amplitudes (high cycle and low cycle fatigue). Histograms are presented that show the number of surface microcracks as a function of their length at different fractions of the fatigue life in air and in vacuum. Analysis of data such as microcrack density, mean crack length and major crack length, permit quantitative characterization of the effect of the atmospheric environment on the different stages of the fatigue failure process.

Notation

$\Delta\varepsilon_t$	Strain range
$\Delta\sigma$	Stress range $\sigma_{max} - \sigma_{min}$
ν	Test frequency
R	Load ratio $\sigma_{min}/\sigma_{max}$
N	Number of cycles
N_F	Number of cycles to failure
N_1	Number of cycles to the initiation of the first surface microcrack one grain boundary (g.b.) long
N_2	Number of cycles at which the first microcrack propagates out of its initiation site
δ	Surface microcrack density (number per mm^2)
δ_{max}	Surface microcrack density at failure
a	Surface crack length
$\overline{a}$	Mean surface crack length
a_{max}	Length of the major surface crack

* Laboratoire de Mécanique et Physique des Matériaux U.A. CNRS 863, 86034 Poitiers Cedex, France.

Introduction

It is well known from the early studies of Gough and Sopwith (**1**) that fatigue lives of most metals cycled in air at room temperature are considerably reduced when compared to tests performed in vacuum or in inert gases. However, it is still not clear how the gaseous environments affect the different stages in the process of fatigue failure.

For copper, Wadsworth and Hutchings (**2**) have shown that the reduction in fatigue life is essentially due to the effect of gaseous oxygen; water vapour increases the oxygen action to a certain degree, but it does not play a direct role in fatigue resistance. These results have been confirmed by Hunsche and Neumann in a more recent study (**3**).

The general opinion about gaseous environments is that they have little or no effect on crack nucleation and initial growth, but affect primarily crack propagation (**2**)(**4**)–(**7**). On the other hand, Thompson *et al.* (**8**) and Broom and Nicholson (**9**), for example, expressed the opinion that gaseous environments play a major role in the crack initiation stage.

Grinberg *et al.* (**10**) and Verkin and Grinberg (**11**) have related the influence of vacuum on fatigue failure to the fact that slip is more homogeneous in vacuum, which delays both the initiation and the propagation of fatigue cracks. However, more recently Wang *et al.* (**12**) and Mendez and Violan (**13**) have found that the surface slip features in air and in vacuum exhibit no significant differences when the comparisons are made at the same number of cycles, and that the homogeneous distribution of surface slip marks is only the result of the extended cycling in vacuum, and not its cause.

In the last ten years, by conducting numerous fatigue experiments on copper single crystals (see, for example (**14**)–(**19**)), significant progress has been made in the understanding of cyclic behaviour and of microcrack initiation processes in Persistent Slip Bands. Concerning the effect of environment, some authors have investigated the fatigue behaviour of copper single crystals in air and in high vacuum or ultra high vacuum (UHV). Wang and Mughrabi (**12**)(**18**)(**20**) have shown that, compared to air, fatigue life was 15 to 30 times greater in high vacuum. Up to the number of cycles to failure in air, the cyclic deformation behaviour in air and in vacuum were similar, however, continuing fatigue in vacuum led to a secondary cyclic hardening stage and to an homogeneous distribution of surface slips traces. Also the crack growth rates, particularly in Stage I, were observed to be lower in vacuum. Hunsche and Neumann (**3**), by conducting the fatigue tests in air or in oxygen, also demonstrated that the surface topography was not modified by the environmental reactions and that crack growth rates are lower in UHV than in air. Moreover these authors found evidence that the fatigue behaviour in vacuum was associated with rewelding.

On the other hand, only a few studies have been done on the effect of environment on polycrystalline copper. However, it is well known that intergranular crack initiation frequently occurs in low cycle fatigue tests (**21**) and sometimes in high cycle fatigue tests (**22**)(**23**).

The aim of the present work is to obtain quantitative information about initiation and growth of small surface intergranular microcracks in air and in vacuum in a fine-grained OFHC copper, in order to characterize the effect of the atmospheric environment on the fatigue damage process during different stages of the lifetime.

Experimental procedure

Fatigue specimens were machined from commercial polycrystalline OFHC copper bars of 22 mm diameter.

Two types of specimens were used: (a) specimens of square cross section with widths of about 6 mm and a gauge length of 16 mm (these specimens were used in total strain controlled tests); (b) specimens with cylindrical gauge lengths 6 mm long and 6 mm in diameter, which were used in load-controlled tests. The specimens were annealed under vacuum for 3 h at 460°C, giving a mean grain size of 30 μm; all the specimens were electropolished before annealing and once again just before the fatigue test. The tests were carried out in a total strain control mode at an amplitude of $\Delta\varepsilon_t/2 = 3.2 \times 10^{-3}$ and a frequency of $\nu = 0.1$ Hz, or in a load control mode using amplitudes varying between 86 and 115 MPa with a frequency $\nu = 37$ Hz and a load ratio $R = -0.95$. The tests were performed at room temperature in air or in a vacuum better than 10^{-3} Pa, using a servo-hydraulic testing machine equipped with a vacuum chamber.

Fatigue specimens were cycled up to failure, or with periodic interruptions to permit their examination by scanning electron microscopy (SEM). At each interruption a quantitative characterization of the fatigue damage was established by determining the number of surface microcracks per unit area (1 mm^2) and by making an estimation of their length.

The method used to evaluate the intergranular microcrack length in the case of fine grained specimens has been indicated elsewhere (**24**). The length of each intergranular microcrack has been estimated by counting the number of grain boundary segments related to the microcrack at the specimen surface. For specimens with a mean grain diameter of 30 μm, the mean length of the grain boundary segments is 0.012 mm. This method is illustrated in Fig. 1 where class 3 indicates three cracked boundaries.

From these measurements we have established histograms for each test condition (amplitude, environment) which give the number of microcracks, in each class of length, at various fractions of the fatigue life. The quantitative analysis of these histograms permits a characterization of the role of environment during the early stages of fatigue damage.

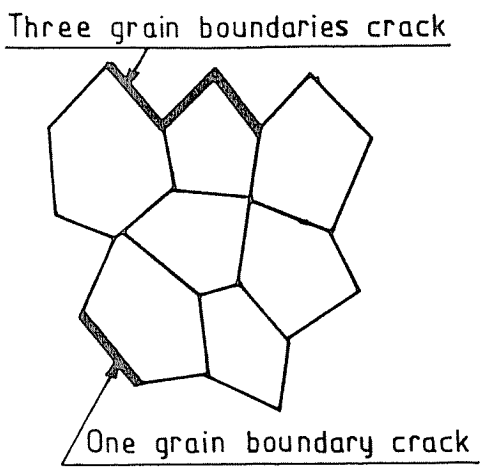

Fig 1 The fatigue damage at the specimen surface is characterized at different fractions of the fatigue life in air and in vacuum by the number of intergranular microcracks per square millimeter and by their length estimated as the number of cracked grain boundary segments

Results and discussion

Fatigue life and crack initiation mechanisms

The fatigue life, the nature of crack initiation sites, and the propagation modes in air and in vacuum for the fine-grained copper investigated here, are listed in Table 1 which classifies the three main test series previously described into class A, class B, and class C.

Table 1 Fatigue life, crack initiation sites, and propagation modes in air and in vacuum for different cyclic loading conditions

Test conditions		N_F *cycles*	*Initiation site*	*Propagation mode*	$\frac{N_{F,vac}}{N_{F,air}}$
Class A					
$\Delta\varepsilon_t/2 = 3.2 \times 10^{-3}$	Air	7.2×10^3	g.b.	Inter	6
$\nu = 0.1$ Hz	Vac.	4.4×10^4	g.b.	Inter	
Class B					
$\Delta\sigma/2 = 115$ MPa	Air	3.25×10^5	g.b.	Inter→Trans	6.5
$R = -0.95$					
$\nu = 37$ Hz	Vac.	2.12×10^6	g.b.	Inter→Trans	
Class C					
$\Delta\sigma/2 = 86$ MPa	Air	5×10^6	PSB	Trans	>11
$R = -0.95$					(≈20)
$\nu = 37$ Hz	Vac.	53×10^6	g.b.	Inter (→Trans?)	

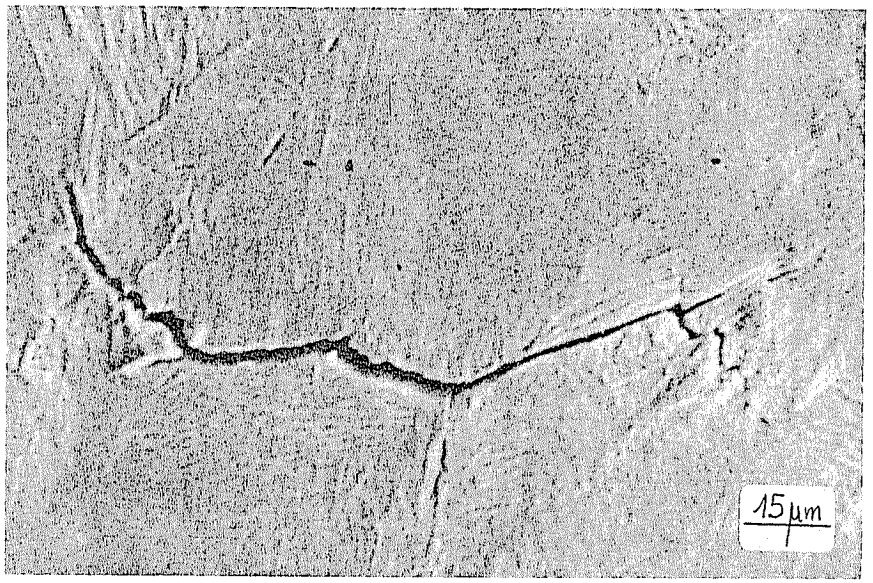

Fig 2 SEM photograph of a secondary surface crack on a specimen tested in air under load amplitude control, $\Delta\sigma/2 = 115$ MPa (test conditions B). Microcracks form early and grow at grain boundaries then start propagating transgranularly

The effect of the environment on fatigue life is significant even for high amplitudes, and especially so in the lowest stress amplitude range (class C) where the ratio $N_{F,vac}/N_{F,air}$ is much higher than 11. The test performed in vacuum at $\Delta\sigma/2 = 86$ MPa was stopped before failure, at 53×10^6 cycles; the examination of the free surface by SEM revealed a major crack only 10 grain boundary (g.b.) segments long ($a \approx 120$ µm), thus indicating an important residual life. From other results obtained in vacuum, at the same stress amplitude, but in coarse-grained specimens ($d = 0.5$ mm) (**25**), it can be assumed that in class C the residual life in vacuum can be about 30 to 50×10^6 cycles leading to $N_{F,vac}/N_{F,air} \approx 20$.

Let us consider now the mechanisms of crack initiation and propagation.

At the highest stress amplitude, class A tests, initiation and propagation of surface microcracks take place at grain boundaries in air as in vacuum. The deformation is uniformly distributed in the grains and few transgranular microcracks are initiated. At the intermediate stress level of 115 MPa, class B tests, microcracks also initiate and propagate early at grain boundaries, but in air this propagation changes to transgranular after a length of 4–6 g.b. segments. In this case, microcracks are also created in Persistent Slip Bands (PSB), in air as in vacuum, but they remain confined inside a grain and do not play any role in the initiation of the main cracks.

At the lowest stress level of 86 MPa, class C tests, crack initiation sites are

different in air and in vacuum. In air our observations are in agreement with those of Thompson *et al.* (**8**) who have shown that, in high cycle fatigue, microcracks initiate in PSBs and propagate transgranularly. On the contrary we have shown that, in vacuum, the initiation and early growth stages always take place at grain boundaries, as for high cyclic loading amplitudes (**13**).

The objective of the present study was to determine the effect of the atmospheric environments on surface crack evolution and so it seemed appropriate to consider only the testing amplitudes leading to identical crack initiation and propagation mechanisms in air and in vacuum. To this effect the studies of microcrack surface features, for example, crack length and density, were only made for the first two test conditions, classes A and B. The interest of comparing quantitative data for these two different cyclic loading amplitudes, low cycle fatigue for the first tests and high cycle fatigue for the second tests, class B, lies in the fact that, in both cases, the same intergranular damage mechanisms are present, and, at the same time, the environmental effect quantified in terms of life ratios is of the same order. At 115 MPa, class B tests, the few transgranular microcracks initiated in air as in vacuum were not taken into account for our quantitative characterization of the fatigue damage. The test at 86 MPa will only be considered here to confirm the tendencies of the environment-induced surface features revealed by comparisons at the higher stress levels, classes A and B.

Histograms of microcrack lengths

Figure 3 shows the results of the measurements performed at different instants of fatigue life in air and in vacuum for the tests corresponding to the highest amplitude of cyclic strains. The histograms giving the number of intergranular microcracks per square millimeter in each class of length have been represented on a linear scale as a function of the number of cycles.

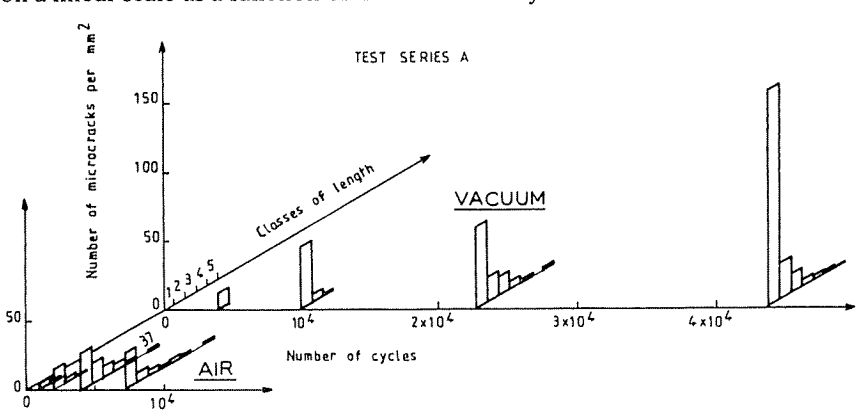

Fig 3 Histograms giving the number of intergranular microcracks per mm² in each class of length for different number of cycles in air and in vacuum. Test class A

The observations were performed using several specimens. First in vacuum a specimen was examined after $N = 1000$ cycles, but no microcrack was observed at this fraction of the fatigue life. The same specimen was cycled again until $N = 4000$ cycles, then $N = 10\,000$ cycles. A second specimen was cycled up to $N = 22\,700$ cycles and a third specimen was directly cycled up to failure ($N_{F,vac} = 43\,700$ cycles).

In air a first specimen was examined at $N = 1000$ cycles and at $N = 2000$ cycles. The second specimen was examined at 4000 cycles and the third completely cycled to failure ($N_{F,air} = 7200$ cycles) before being examined. The second specimen tested until $N = 4000$ cycles in air was continued in vacuum at the same amplitude, leading to a residual fatigue life in vacuum of 10 000 cycles. Therefore, the degree of fatigue damage in air at $N = 4000$ cycles is equivalent to that in vacuum at 34 000 cycles. This result is in agreement with the histograms of Fig. 3; in air at 4000 cycles the maximum crack length is already over 37 g.b. segments, whereas after 22 700 cycles in vacuum it is only seven g.b. segments long.

The histograms in Fig. 4 show the behaviour of small surface cracks in the case of intermediate stress levels, class B tests. These results have been obtained using only one specimen in vacuum and two specimens in air; the first one examined at 5×10^4 cycles then at 10^5 cycles whilst the second one was examined at 1.5×10^5 cycles then at 2.75×10^5 cycles.

A first analysis of Fig. 3 and Fig. 4 shows the following.

(1) the important accelerating effect of air on the processes of initiation and early growth of the small surface cracks. For example at the highest strain level tests, class A, at 10 000 cycles the largest crack in vacuum is only 3 g.b. segments long, whereas in air the specimen fractured at only 7200 cycles. At the intermediate stress level of 115 MPa, class B, the formation

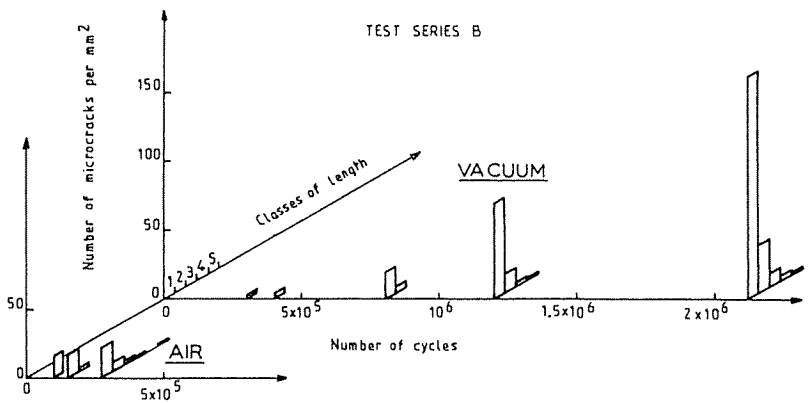

Fig 4 Histograms giving the number of intergranular microcracks per mm² in each class of length at different number of cycles in air and in vacuum. Test class B

of a small surface microcrack 2 g.b. segments long in vacuum requires a greater number of cycles than $N_{F,air}$.

(2) that the prolonged cycling in vacuum leads to the initiation of a much higher number of intergranular microcracks as compared to the fatigue behaviour in air (compare the heights of the histograms corresponding to the specimens cycled at failure in air and in vacuum).

(3) that for all the testing conditions, most of the surface microcracks remain small; their length on the fractured specimens being smaller than 5 or 6 g.b. segments.

Evolution of microcrack density and mean crack length

Figures 5 and 6 show the increase of the density δ of intergranular microcracks in air and in vacuum with cycling at the two highest stress–strain levels. The values of the different quantities calculated from Fig. 5 and 6 plots, are listed in Table 2.

The extrapolation of the curves δ–N to zero density gives an estimation of the number of cycles N_1 leading to the initiation of first surface microcracks: $N_{1,vac}$ is three times higher than $N_{1,air}$ in class A tests and about five times higher in class B tests.

From the curves δ–N the effect of the environment can also be characterized by differences obtained in the rate of initiation of new microcracks. In class A tests, Fig. 5 shows that δ increases linearly with the number of cycles in air, as in vacuum, with a slope, $\Delta\delta/\Delta N$, three times lower in vacuum than in air.

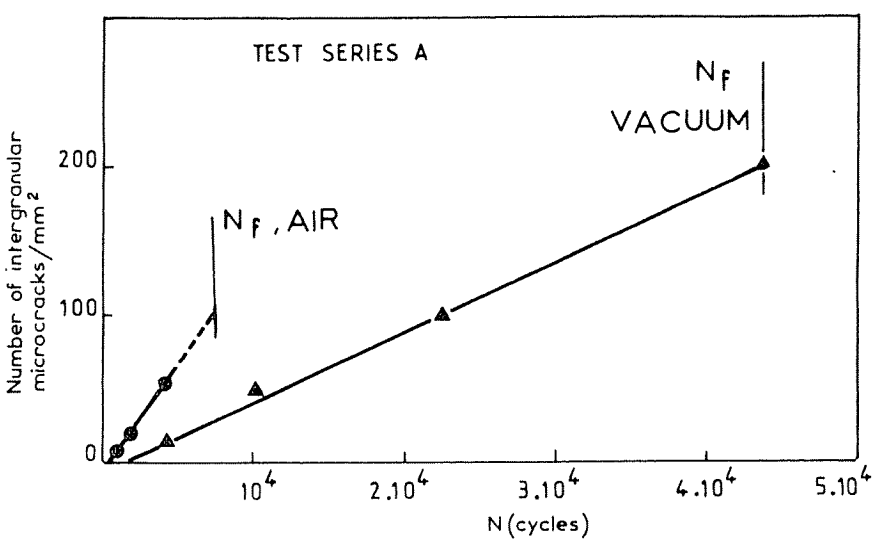

Fig 5 Evolution of the microcrack density as a function of the number of cycles in air and in vacuum for the test series A (high amplitudes)

Table 2 Number of cycles leading to the initiation of the first microcracks (N_1), rate of initiation of new microcracks, and maximum density

Test conditions		N_1 *cycles*	N_1/N_F	$\Delta\delta/\Delta N$ *microcracks per cycle*	δ_{max} *microcracks per mm²*
Class A $\Delta\varepsilon_t/2 = 3.2 \times 10^{-3}$	Air	500	0.07	1.5×10^{-2}	56
	Vac.	1400	0.03	4.8×10^{3}	200
Class B $\Delta\sigma/2 = 115$ MPa	Air	5×10^{4}	0.15	1.3×10^{-4}	32
	Vac.	1.5×10^{5}	0.07	0.45 then 1.5×10^{-4}	218

For class B tests in air a similar behaviour is found, but the results obtained in vacuum exhibit two distinct domains as indicated by two straight line plots. The slope $\Delta\delta/\Delta N$ is three times lower in vacuum than in air in the first part of the test, but reaches a value as high as in air in the latter part of the test.

Another important characteristic of the environmental effect is the difference between the maximum microcrack density values δ_{max} reached in air and in vacuum, both in low cycle and in high cycle fatigue ranges. One can see from Table 2 that δ_{max} is four times higher in vacuum than in air in class A tests and six times higher in class B tests. Moreover, the differences in δ_{max} because of the environment are still more striking for the lower stress levels of class C tests (see

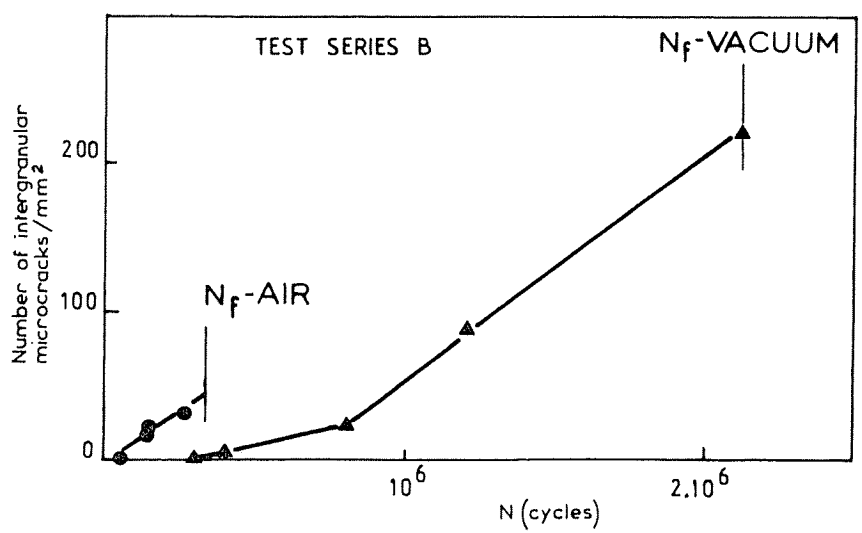

Fig 6 Evolution of the microcrack density as a function of the number of cycles in air and in vacuum for test series B (low amplitudes)

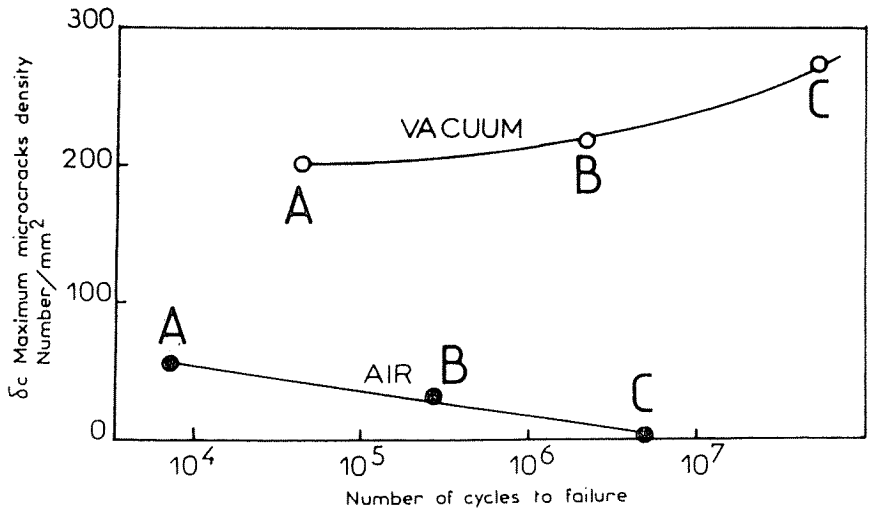

Fig 7 Plots of the maximum density of intergranular initiated microcracks in air and in vacuum as a function of the number of cycles to fracture for test series A, B, and C

Table 1). In this case we found a microcrack density of 270 microcracks per mm^2 in vacuum, higher than for class A and class B tests, although the measurements were made before the specimen fractured. In air, however, the microcrack density, in PSBs or grain boundaries, is very low, just a few microcracks per square millimeter. In Fig. 7, we have plotted δ_{max} against N_F in air and in vacuum from the curves of δ against N obtained for the test classes A, B, and C.

The evolution of δ_{max} observed in air is a similar result to that obtained by other authors on different materials (see, for instance, (**26**) and (**27**)). In air the fatigue damage process becomes more and more heterogeneous as the fatigue life increases. This behaviour is not observed in vacuum; on the contrary, Fig. 7 shows that in this environment δ_{max} tends to increase slightly with N_F. Thus it appears that in vacuum the coalescence of small cracks could play an important role in the formation of the main crack, whatever the cyclic loading amplitudes. This is not so in air, particularly at low stress amplitudes.

Figure 8 shows the evolution of the mean value of the crack length, $\bar{a}$, at the specimen surface, calculated from the measurements that produced histograms of the Figs 3 and 4. The extrapolation of the experimental curves $\bar{a}$ to the value $\bar{a} = 1$ g.b. segment gives an estimation of the number of cycles, N_2, beyond which $\bar{a}$ becomes higher than 1 g.b. segment; in other words it is considered that at N_2 the first microcracks start spreading out from their initiation sites into the neighbouring grains.

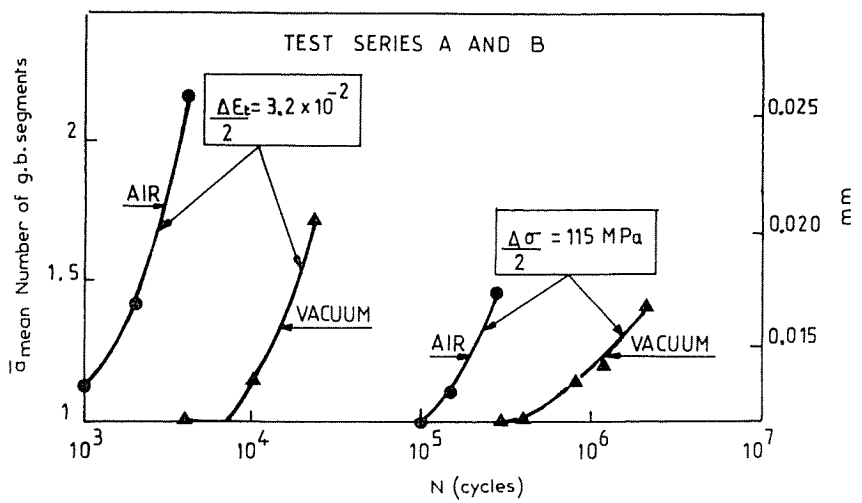

Fig 8 Evolution of the mean crack length $\bar{a}$ in air and in vacuum as a function of the number of cycles for test series A and B

The values of N_2 determined from the $\bar{a}$–N curves are given in Table 3. The effect of the environment on this stage of fatigue damage is more important for the high amplitude than for the low amplitude tests. Moreover, it is interesting to note that in the class B tests the effect of the environment is higher on N_2 than on the total fatigue life. However, in the class B tests our results are more in agreement with the general belief according to which the effect of environment concerns particularly crack propagation. The $\bar{a}$–N plots also clearly show that for all the test conditions of stress and environment, the majority of the intergranular cracks remain very small during the specimen life since the mean crack length stays lower than 30 μm.

Table 3 Number of cycles leading to the propagation of the first microcrack out of its initiation site (N_2)

Test classes	*Environment*	N_2 (*cycles*)	*Ratio*
A	Air	800	8.75
	Vac.	7000	
B	Air	10^5	4
	Vac.	4.10^5	

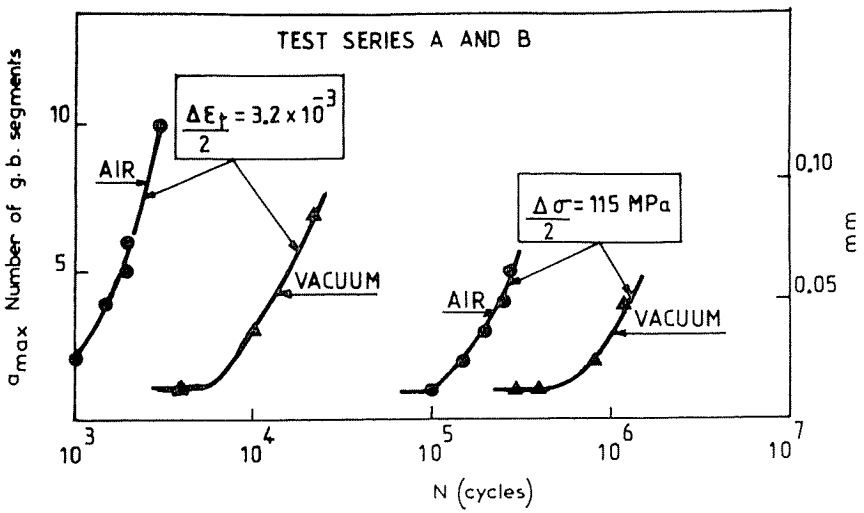

Fig 9 Evolution in the early stages of damage of the major crack length a_{max} versus the number of cycles in air and in vacuum. Test series A and B

The increase of the major crack length in the early stages of microcrack growth

The length of the largest surface crack observed at different number of cycles in air and in vacuum for the class A and B tests conditions has been plotted as a function of the number of cycles N in Fig. 9 and as a function of N/N_F in Fig. 10, with a linear scale. In these plots it has been taken into account that the crack only starts propagating at the number of cycles, N_2, previously defined. The fatigue behaviour investigated here concerns the very early stage of microcrack development in which the major crack length involves only a few boundary segments ($a_{max} \approx 100$ μm). In this range of small crack length the evolution of a_{max} versus N can be described by linear plots as it can be seen in Fig. 10.

An estimation of the growth rates at the specimen surface in this micro-propagation stage suggests the values given in Table 4. In this table are also

Table 4 Propagation rate in the first stages of microcrack development ($a_{max} \approx 100$ μm) and number of cycles of propagation in air and in vacuum

Test classes	*Environment*	*da/dN (mm/cycle)*	*Ratio*	$N_F - N_2$ *(cycles)*	*Ratio*
A	Air	$3.50\ 10^{-5}$	6.4	6400	5.8
	Vac.	$5.45\ 10^{-6}$		37000	
B	Air	$2.40\ 10^{-7}$	5.8	225000	7.6
	Vac.	$4.14\ 10^{-8}$		1720000	

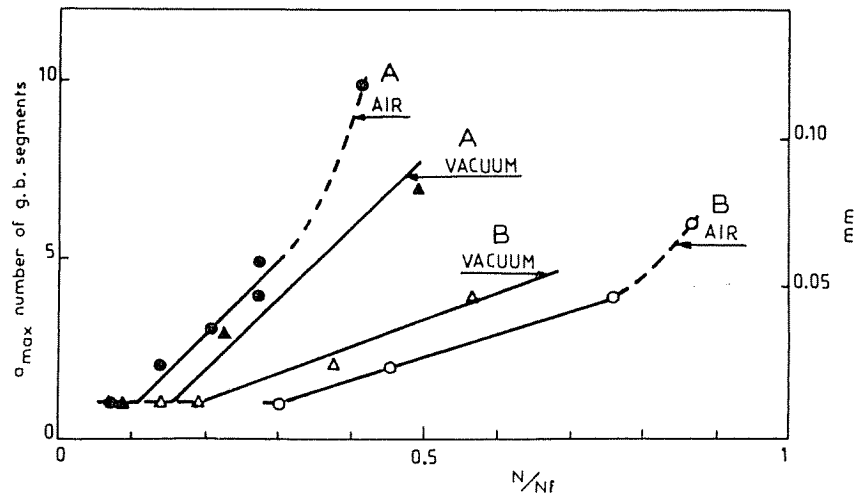

Fig 10 Evolution of the major crack length a_{max} plotted versus the fraction of the fatigue life. Test series A and B

listed the number of cycles ($N_F - N_2$) corresponding to the duration of the whole propagation stage. Our results on the effect of environment on the growth rates of very small surface cracks are in opposition to the usual opinion, according to which the lower the propagation rate, the higher the environmental effect. Indeed, it must be noted that the rates measured in class A tests are more than 100 times higher than in class B tests.

On the other hand, from the comparisons between the curves in Fig. 10 giving a_{max} as a function of the fraction of lifetime, and from the values of N_2 reported in Table 3, the following features were noted.

(1) In air, the well known behaviour according to which crack initiation occurs earlier in life for low cycle than for high cycle fatigue is verified. The first microcracks start propagating at $N_2/N_F = 0.11$ during class A tests and at $N_2/N_f = 0.31$ for class B tests. Moreover, the early stages of the major crack development take a small fraction of the fatigue life in class A tests, but a very significant fraction of the fatigue life in class B tests. For example, for a major crack length of 4 g.b. segments, $N/N_F = 0.25$ for class A tests but 0.8 for class B tests.

(2) In vacuum, a similar behaviour is found; however, from one test to another, the differences in the fatigue life fractions occupied by the initiation and the early development of the microcracks are less marked than in air. The first microcracks start propagating at $N_2/N_F = 0.16$ for class A tests and $N_2/N_F = 0.19$ for class B tests, and for a major crack

length of 4 g.b. segments the fatigue life fractions are, respectively, 0.3 and 0.6.

(3) The relative positions of the air and vacuum curves are different for the test classes A and B. For the class A series (Low Cycle Fatigue) Fig. 10 shows that the curve $\mathbf{a}_{max}$ in air is at lower values of N/N_F than that for vacuum, while for the class B tests, the curve for air is at higher values of N/N_F.

From points (1) and (2) above one can see that the crack initiation occurs early in the fatigue life for high amplitude tests. That this is verified in vacuum as well as in air clearly shows that this behaviour is characteristic of low cycle fatigue, whatever the environment. However, the opinion that the crack initiation stage takes a larger fraction of the fatigue life for low amplitude than for high amplitude fatigue tests is verified in air more than in vacuum. Therefore this behaviour appears typical of environment-affected fatigue damage processes. In vacuum the fraction of the fatigue life associated with propagation remains important in high cycle fatigue tests.

The third point concerning the relative position of the curves a_{max}–(N/N_F) in air and in vacuum, see Fig. 10, shows that in low cycle fatigue the effect of the environment is important for the initiation and early growth of very small cracks ($a \approx 100$, μm) compared to the later stages of fatigue damage. However, in the case of high cycle fatigue, the environmental effect appears to be less in the early stages of fatigue damage than in the subsequent stages.

Let us summarize now the effect of the environment on the different stages of fatigue damage considered in this study. Concerning the class A tests, the effect of environment is especially marked on the stage characterized by the number of cycles $(N_2 - N_1)$ which leads from the formation of the first surface microcracks one grain boundary long (N_1) to the beginning of the stage of propagation (N_2); we found a ratio of 18 between the tests in vacuum and in air. On the contrary, the effect on N_1 is weak, only a ratio of 3. We have also found that the environmental effect is greater on the micropropagation stage, leading to a surface microcrack of a few grain boundary segments long, than in the later stages of propagation, see Table 4. Thus it is easy to understand that the environmental effect is less during the later crack propagation stages where the crack growth rates are higher.

More surprising are the results in class B tests (low amplitudes) where the effects of the environment become higher in the propagation stages following the formation of a microcrack 5 or 6 g.b. segments long: indeed,we have found a ratio of 5 between $(N_2 - N_1)$ values in vacuum and in air and a ratio of 5.8 between the characteristics of the micropropagation stage. Note that the global effect on fatigue life is 6, that the effect during all the propagation stage $(N_F - N_2)$ is 7.6, but that the effect on propagation in the stage leading from a microcrack of 4 g.b. segments long to specimen failure is as high as 13. The difference in this case, compared to the test series A, is the occurrence of a

transition from an intergranular crack propagation mode to a transgranular one at microcrack lengths of about 5–6 g.b. segments. Thus, our results tend to prove that the effect of environment is more marked on transgranular propagation than on intergranular propagation. This behaviour is in good agreement with previous work by Violan *et al.* (**28**) on polycrystalline OFHC copper which gave a ratio of 17 between the mean crack growth rates in air and in vacuum.

Another result which appears very surprising at first sight is that the influence of the environment during the first stages of fatigue damage is higher for the high amplitude levels than for the lower amplitudes, although for both cases this stage corresponds to the same microcrack length (up to 5 or 6 g.b. segments). However, in interpreting these results, one must take into account the differences in testing frequencies (370 times lower in test series A). It is well known that the effect of an aggressive environment on fatigue crack propagation increases when the test frequency decreases (see, for example, (**29**) and (**30**).

Conclusions

The initiation and early growth of intergranular surface fatigue microcracks in air and in vacuum have been studied in a fine-grained OFHC copper under different loading conditions which leads to the following main conclusions.

(1) Prolonged cycling in vacuum, in both high cycle and low cycle fatigue, leads to the initiation of a greater number of surface microcracks than in air.

(2) Atmospheric environment has a significant effect on the initiation period leading to the formation of a microcrack one grain boundary segment long. However, this effect is less than the environmental effect on the total fatigue life.

(3) In the case of high cyclic amplitudes, environment mainly affects the subsequent fatigue damage stages, until the formation of a microcrack about 100 μm long. This behaviour appears to be related to the low frequencies used during the present tests.

(4) In low amplitude fatigue tests the effect of environment appears to be much more marked in the crack propagation stage following the formation of intergranular microcracks 5 or 6 grain boundary segments long. This behaviour is associated with a change in crack propagation mode from intergranular to transgranular.

References

(1) GOUGH, H. J. and SOPWITH, D. C. (1932) Atmospheric action as a factor in fatigue of metals, *J. Inst. Metals*, **49**, 92–112.

(2) WADSWORTH, N. J. and HUTCHINGS, J. (1958) The effect of atmospheric corrosion on metal fatigue, *Phil. Mag.*, **3**, 1154–1166.

(3) HUNSCHE, A. and NEUMANN, P. (1984) Crack nucleation in persistent slip bands,

ASTM Symposium *Fundamental Questions and Critical Experiments on Fatigue*, Dallas, October, 1984, to be published as ASTM Special Technical Publication.

(4) LAIRD, C. and SMITH, G. C. (1963) Initial stages of damage in high stress fatigue in some pure metals, *Phil. Mag.*, **8**, 1945–1963.

(5) ACHTER, M. R. (1967) Effect of environment on fatigue cracks, *Fatigue crack Propagation, ASTM STP 415* (American Society for Testing and Materials, Philadelphia), pp. 181–204.

(6) LAIRD, C. and DUQUETTE, D. J. (1972) Mechanisms of fatigue crack nucleation, *Corros. Fatigue*, **NACE-2**, 88–117.

(7) DUQUETTE, D. J. (1979) Environmental Effects I: General fatigue resistance and crack nucleation in metals and alloys, *Fatigue and microstructure* (American Society for Metals), pp. 335–363.

(8) THOMPSON, N., WADSWORTH, N. J., and LOUAT, N. (1956) The origin of fatigue fracture in copper, *Phil. Mag.*, **1**, 113–126.

(9) BROOM, T. and NICHOLSON, A. (1961) Atmospheric corrosion-fatigue of age-hardened aluminium alloys, *J. Inst. Metals*, **89**, 183–190.

(10) GRINBERG, N. M., ALEKSEYEV, A. I., and LYUBARSKI, I. M. (1972) Influence of vacuum on the various stages in the fatigue failure of copper, *Fiz. Metal. Metalloved*, **34**, 1259–1263.

(11) VERKIN, B. I. and GRINBERG, N. M. (1979) The effect of vacuum on the fatigue behaviour of metals and alloys, *Mater. Sci. Engng*, **41**, 149–181.

(12) WANG, R., MUGHRABI, H., McGOVERN, S., and RAPP, M. (1984) Fatigue of copper single crystals in vacuum and in air I: Persistent Slip Bands and dislocation microstructure, *Mater. Sci. Engng*, **65**, 219–233.

(13) MENDEZ, J. and VIOLAN, P. (1984) Modifications in fatigue damage processes induced by atmospheric environment in polycrystalline copper, ASTM Symposium *Fundamental questions and critical experiments on fatigue*, Dallas, October 1984, to be published as ASTM Special Technical publication.

(14) WINTER, A. T. (1974) A model for the fatigue of copper at low plastic strain amplitudes, *Phil. Mag.*, **30**, 719–738.

(15) MUGHRABI, H. (1978) The cyclic hardening and saturation behaviour of copper single crystals, *Mater. Sci. Engng*, **33**, 207–223.

(16) BASINSKI, Z. S. KORBEL, A. S., and BASINSKI, S. J. (1980) The temperature dependence of the saturation stress and dislocations substructure in fatigue copper single crystals, *Acta. Met.*, **28**, 191–208.

(17) CHENG, A. S. and LAIRD, C. (1981) Fatigue life behaviour of copper single crystals. Part I: observations of crack nucleation; Part II: model for crack nucleation in persistent slip bands, *Fatigue Engng Mater. Structures*, **4**, 331–342; 343–354.

(18) WANG, R. and MUGHRABI, H. (1984) Secondary cyclic hardening in fatigued copper monocrystals and polycrystals, *Mater. Sci. Engng*, **63**, 147–164.

(19) BASINSKI Z. S. and BASINSKI, S. J. (1985) Low amplitude fatigue of copper single crystals: II – Surface observations; III – PSB sections, *Acta Met.*, **33**, 1307–1318; 1319–1328.

(20) WANG, R. and MUGHRABI, H. (1984) Fatigue of copper single crystals in vacuum and in air. II: Fatigue crack propagation, *Mater. Sci. Engng*, **65**, 235–244.

(21) KIM, W. H. and LAIRD, C. (1978) Crack nucleation and Stage I propagation in high strain fatigue – I: Microscopic and interferometric observations; II: Mechanism, *Acta Met.*, **26**, 777–788; 789–800.

(22) FIGUEROA, J. C. and LAIRD, C. (1978) Crack initiation mechanisms in copper polycrystals cycled under constant strain amplitudes and in step tests, *Mater. Sci. Engng*, **60**, 45–58.

(23) MUGHRABI, H. (1983) A model of high-cycle fatigue crack initiation at grain boundaries by persistent slip bands, *Defects, fracture, and fatigue*, Edited by G. C. Sih and J. W. Provan (Martinus Nijhoff, The Hague) pp. 139–140.

(24) MENDEZ, J., VIOLAN, P., and GASC, C. (1984) Characterization of fatigue processes in a fine-grained copper tested in air and in vacuum, *Life assessment of dynamically loaded materials and structures*, Edited by L. Favia, Lisbon Vol. 1, pp. 515–522.

(25) MENDEZ, J. (1984) *Etude comparative des mécanismes d'amorçage des microfissures de fatigue sous air et sous vide dans le cuivre polycristallin. Influence d'une implantation ionique*, Thèse de Doctorat, Poitiers, France.

(26) KITAGAWA, H., TAKAHASHI, S., SUH, C. M., and MIYASHITA, S. (1979) Quantitative analysis of fatigue process-Microcracks and slip lines under cyclic strains, *Fatigue Mechanisms, ASTM STP 675*, Edited by J. T. Fong (American Society for Testing and Materials), pp. 420–449.

(27) SUH, C. M. YUUKI, R., and KITAGAWA, H. (1985) Fatigue microcrack in a low carbon steel, *Fatigue Fract. Engng Mater. Structures*, **8**, 193–203.

(28) VIOLAN, P., COUVRAT, P., and GASC, C. (1979) Influence of crystalline orientation on the environment affected fatigue crack propagation in copper, *Strength of metals and alloys*, Edited by P. Haasen and V. Gerold (Pergamon Press, New York) Vol. 5, pp. 1189–1194.

(29) COFFIN, L., Jr (1972) The effect of high vacuum on the low cycle fatigue law, *Met. Trans*, **3**, 1777–1788.

(30) BIGONNET, A., LOISON, D., NANDAR-IRANI, R., BOUCHET, B., KWON, J. H., and PETIT, J. (1983) Environmental and frequency effects on near-threshold fatigue crack propagation in a structural steel, *Fatigue crack growth threshold concepts*, Edited by Davidson and Suresh (The Metallurgical Society of AIME), pp. 99–114.